Journal of Materials Chemistry B

Accepted Manuscript

ROYAL SOCIETY OF CHEMISTRY

www.rsc.org/materialsB

Journal of Materials Chemistry B RSCPublishing

ARTICLE

Photolinker-free photoimmobilization of antibodies onto cellulose for the preparation of immunoassay membranes

Julie Credou,[a] Hervé Volland[b] and Thomas Berthelot[a]* ,

Cite this: DOI: 10.1039/x0xx00000x

Received ooth July 2014,
Accepted ooth July 2014

DOI: 10.1039/x0xx00000x

www.rsc.org/

Paper-based detection devices such as lateral flow immunoassays (LFIAs) are inexpensive, rapid, user-friendly and therefore highly promising for providing resource-limited settings with point-of-care diagnostics. Recently, this biosensing field has trended towards three-dimensional microfluidic devices and multiplexed assay platforms. However, many multiplexed paper-based biosensors implement methods incompatible with the conventional LFIA carrier material: nitrocellulose. It thus tends to be replaced by cellulose. This major material change implies to undertake a covalent immobilization of biomolecules onto cellulose which preserves their biological activity. In this perspective, the immobilization process elaborated in this study is entirely biocompatible. While antibody immobilization onto cellulose usually requires chemical modifications of either the biomolecule and/or the membrane, the light-based procedure presented here was performed without any chemical photolinker. Native biomolecules have been successfully immobilized onto paper sheets which therefore enable to perform LFIAs. More generally, the process expounded herein is fast, simple, cost-saving, environmentally-friendly and would be helpful to immobilize chemical-sensitive biomolecules onto cellulose sheets.

1. Introduction

In various domains such as clinical diagnosis [1–5], drug screening [6–9], food quality control [10–12], and environmental monitoring [13–16], there is a need to easily and rapidly detect biomolecules. Several methods have been developed for manufacturing biosensors, biochips, microarray and other immunoassay devices [17,18,7,19–22]. Within the last thirty years, paper-based biosensors such as lateral flow assays have attracted a strong interest and were extensively developed [23–25]. Among these, blood glucose sensors, pregnancy tests, or urine test strips are the most broadly distributed devices for identifying biomolecules [26,25,27–32].

The preparation of such efficient immunoassay devices requires the robust immobilization of a large number of biomolecules of interest on a support [33]. Because of its ability to immobilize all kind of proteins by a combination of electrostatic, hydrogen, and hydrophobic interactions involving the nitro functions displayed on its surface [28], nitrocellulose constitutes the most commonly used support material for preparing immunochromatographic devices [27,25,28,34]. However, nitrocellulose is an expensive, fragile and inflammable material [35,36], which was shown to be incompatible with newly developed multiplex biosensors such as lab-on-paper devices, microfluidic paper analytical devices (μPADs), or other paper-based analytical devices [21,7,37]. Moreover, some agents such as spores and some bacteria may have difficulty in migrating along nitrocellulose. For these reasons, nitrocellulose is thus progressively replaced by cellulose [37,38].

Cellulose is an affordable biopolymer, which is also biocompatible, biodegradable and easily available [39–42]. It is particularly interesting since it exhibits wicking properties allowing biomolecules in solution to migrate by capillarity without needing any external power sources. It is also available in a broad range of thickness and possesses well-defined pore sizes, is easy to store and safely disposable [37]. Several methods for immobilizing biomolecules onto cellulose are known. They may be classified into three major families: (i) physical methods, wherein the biomolecule is confined to the support through physical forces such as electrostatic, Van der Waals and hydrophobic interactions; (ii) biological or biochemical methods wherein the biomolecule is bound to the support through biochemical affinity between two components (*e.g.* Ni^{2+} / His-tag, streptavidin / biotin, protein G / human IgG); and (iii) chemical methods, wherein covalent bonds link the biomolecule on the support [38]. Nevertheless, each of these methods also displays specific drawbacks. Physical methods implement simple, rapid and cost-saving procedures, and

advantageously limit the necessity for modifying the biomolecule or the support. However, the weak and non-permanent interaction maintaining the biomolecule onto the support also represent a major drawback of these methods, since biomolecules are progressively torn out, thus triggering a loss of activity of the corresponding biosensor. Biological methods allow biomolecules to be immobilized in a specific orientation through strong, specific and reversible interactions with the support. Nevertheless, these methods require complex and expensive engineering procedures wherein the biomolecule and/or the support are modified for introducing a binding conjugate or a binding domain therein. Finally, chemical methods ensure strong, stable and permanent coupling of the biomolecule to its support. The thus-conceived biosensors are robust and provide reproducible results. On the other hand, the chemical treatments performed may modify and alter the structure and/or the activity of the biomolecules. The resulting biosensors may thus lack sensitivity as a consequence of biomolecule alteration.

Among the known covalent coupling techniques, photoimmobilization is probably the simplest and the fastest for preparing bioassay devices. The support is usually coated or functionalized with a photoreactive compound and the biomolecule of interest is covalently linked to the support through photoactivation of the latter. Given that short-wave UV (ultraviolet) light (*i.e.* 100 nm - 340 nm) is known to alter biomolecules [43], photoimmobilization is then generally performed under long-wave UV light (340 nm – 400 nm) or visible light (400 nm - 800 nm) [44–46]. To the best of our knowledge all the photoimmobilization methods described so far have required a photoreactive coupling intermediate [37,47–50] and further functionalization of cellulose through harsh conditions, in organic solvents, or with highly toxic reagents or side products [37]. There is therefore an ongoing need for cost-saving and rapid methods allowing immunoassay devices to be prepared by robust and sustainable binding of biomolecules to cellulose. There is indeed a long-felt need for unmodified antibody immobilization methods displaying a limited number of steps, allowing to save significant amounts of reagents, solvents or adjuvants, and ensuring the preservation of the activity of the biomolecules of interest through the use of mild conditions.

The new process developed and presented herein actually fulfills this need. This is a photolinker-free photografting procedure which allows biomolecules to be immobilized onto cellulose without any photocoupling intermediate nor any biomolecule or substrate pretreatment [51]. This is therefore a fast, simple, cost-saving and environmentally-friendly method for native antibody immobilization onto cellulose. The procedure can be summarized as follows: (i) a cellulose sheet was impregnated with an antibody solution; (ii) antibodies were optionally concentrated by drying the impregnated paper; (iii) the system was irradiated for inducing photoimmobilization; and (iv) intensive washing was performed for removing non-immobilized antibodies. After a saturation step aiming at preventing further nonspecific protein adsorption, the so prepared membranes were used as detection zone in lateral flow immunoassays (LFIAs). In these assays, the model antigen selected to validate our procedure was ovalbumin (OVA), and the antibodies directed against its epitopes were murine monoclonal antibodies. Each membrane was subjected to two classes of assay. The first one evaluated the immobilization rate and the second one the biological activity rate. For each membrane, 2 or 3 different samples were tested, depending on the experiment. All results were analyzed with respect to nitrocellulose as the positive control and to pristine unirradiated cellulose paper as the negative control regarding protein immobilization. Various parameters of the photoimmobilization process have thus been optimized, therefore resulting in an optimal procedure which produces membranes challenging nitrocellulose performances.

2. Experimental

2.1. Reagents and materials

Papers used for performing the immunoassay membranes comprise celluloses CF1 and Chr1, as well as AE 98 Fast nitrocellulose from Whatman (Maidstone, Kent, UK) and printing paper Xerox Premier 80 (Ref. 3R91720, Xerox, Norwalk, CT, USA). Immunochromatographic strips were prepared using Standard 14 sample wick from Whatman (Maidstone, Kent, UK), No. 470 absorbent pad from Schleicher and Schuell BioScience GmBH (Dassel, Germany) and MIBA-020 backing card from Diagnostic Consulting Network (Carlsbad, CA, USA). Materials were cut using an automatic programmable cutter Guillotine Cutting CM4000 Batch cutting system from BioDot (Irvine, CA, USA). Antibody solutions were either dropped onto substrates using a pipette, or dispensed at 1 $\mu L\ cm^{-1}$ using an automatic dispenser (XYZ3050 configured with 2 BioJet Quanti Dispenser (BioDot, Irvine, CA, USA)).

Proteins (ovalbumin (OVA), Bovine Serum Albumin (BSA) and porcine skin gelatin), as well as chemical products for preparing buffers and colloidal gold solution were obtained from Sigma-Aldrich (St Louis, MO, USA). Water used in all experiments was purified by the Milli-Q system (Millipore, Brussels, Belgium). Monoclonal murine antibodies (murine mAbs) were produced at LERI (CEA, Saclay, France) as previously described [52].

Irradiations were conducted at room temperature in a UV chamber CN-15.LV UV viewing cabinet (Vilber Lourmat, Marne-la-Vallée, France). 96-Well polystyrene microplates (flat-bottom, crystal-clear, from Greiner Bio-One S.A.S. Division Bioscience, Les Ulis, France) were used as container for migrations on immunochromatographic strips. Colorimetric intensity resulting from colloidal gold was quantified with a Molecular Imager VersaDoc^{TM} MP4000, in association with the software Quantity One 1-D Analysis (Bio-Rad, Hercules, CA, USA).

2.2. Photoimmobilization of antibodies

2.2.1. General procedure

Murine monoclonal antibodies directed against OVA epitopes (1 mg mL^{-1} in 0.1 M potassium phosphate buffer, pH 7.4, 40 µL cm^{-2} deposit) were photoimmobilized onto pristine CF1 cellulose paper. They also were adsorbed onto nitrocellulose (positive control) and onto pristine CF1 cellulose paper (negative control) by regular 1-hour incubation at room temperature. Results obtained after photoimmobilization were compared to positive and negative controls.

Photoimmobilization process can be briefly described as follows: (i) a cellulose sheet was impregnated with an antibody solution; (ii) antibodies were optionally concentrated by drying the impregnated paper; (iii) the system was irradiated for inducing photoimmobilization; and (iv) intensive washing was performed for removing non-immobilized antibodies. For each membrane, an anti-OVA antibody solution was dropped onto a 0.25-cm^2 cellulose sheet (0.5 cm x 0.5 cm in size) at a rate of 40 µL cm^{-2}. Where applicable, drying was performed at 37°C, in a ventilated oven, for 15 minutes. Irradiation was either conducted at 365 nm (1050 µW cm^{-2}) or in visible light (power characteristics not provided). After irradiation, samples were washed with 0.1 M potassium phosphate buffer, pH 7.4, optionally enriched with salts (0.5 M NaCl) and detergent (0.5% (v/v) Tween 20).

Membranes were then saturated with a gelatin solution (0.1 M potassium phosphate buffer, pH 7.4, containing 0.5% (w/v) porcine gelatin and 0.15 M NaCl) for preventing nonspecific protein adsorption on membranes during immunoassays. Saturation was performed by impregnating and incubating the membranes with the gelatin solution overnight at 4°C, and then drying them at 37°C in a ventilated oven for 30 minutes.

2.2.2. Variable parameters

Various parameters of the photoimmobilization process had been optimized in order to determine an optimal procedure. Therefore, the cellulose carrier impregnated with the antibody solution might either be dried or not before the irradiation step. The light used for irradiating the impregnated cellulose carrier might have a wavelength of 365 nm (long-scale UV) or ranging from 400 nm to 800 nm (visible light). With a wavelength of 365 nm, the irradiations were conducted for various periods of time that subjected the impregnated cellulose carriers to different photoenergies ranging from 1 J cm^{-2} to 80 J cm^{-2}. Finally, the washing phosphate buffer could either be pure or enriched with salts and detergent. The efficiency of each parameter was assessed by the immobilization and activity performances of the prepared membranes which were ascertained by immunochromatographic assays.

2.3. Immunochromatographic assays (LFIA)

Immobilization rate and biological activity rate of the immobilized antibodies were evaluated by colloidal-gold-based lateral flow immunoassays (LFIA) [25]. The signal intensity was quantitatively estimated by colorimetric measurement. All results were compared with adsorption on pristine cellulose (negative control) and nitrocellulose (positive control). Considering that adsorption on nitrocellulose is the most frequently used method for immunochromatographic assays, it is herein considered as the reference and has been assimilated to 100% for both the immobilization rate and the activity rate.

All the reagents were diluted in the analysis buffer (0.1 M potassium phosphate buffer, pH 7.4, containing 0.1% (w/v) BSA, 0.15 M NaCl, and 0.5% (v/v) Tween 20), at room temperature, 30 minutes prior to migration in order to reduce nonspecific binding. Each assay was performed at room temperature by inserting a strip into a well of a 96-well microtiter plate containing 100 µL of the test solution. The mixture was successively absorbed by the various pads and the capillary migration process lasted for about 15 minutes. Colorimetric intensity was further measured using the molecular imager. Since this intensity depended on parameters such as temperature and moisture content of paper at the time of measurement, all strips were dried for 30 minutes at 37°C in a ventilated oven and then rehydrated with the analysis buffer just before measurement [37].

2.3.1. Preparation of colloidal-gold-labeled antibodies

Tracer antibodies were labeled with colloidal gold according to a known method previously described [53]. Two types of tracer were prepared: a goat polyclonal antibody anti-mouse tracer to reveal the immobilized murine antibodies, and a murine monoclonal antibody anti-OVA tracer to highlight the capture of OVA by the immobilized antibodies.

Briefly, 4 mL of gold chloride and 1 mL of 1% (w/v) sodium citrate solution were added to 40 mL of boiling water under constant stirring. Once the mixture had turned purple, this colloidal gold solution was allowed to cool to room temperature and stored at 4°C in the dark. 25 µg of antibody and 100 µL of 20 mM borax buffer, pH 9.3, were added to 1 mL of this colloidal gold solution. This mixture was left to incubate for one hour on a rotary shaker at room temperature, therefore enabling the ionic adsorption of the antibodies onto the surface of the colloidal gold particles. Afterwards, 100 µL of 20 mM borax buffer, pH 9.3, containing 1% (w/v) BSA, was added and the mixture was centrifuged at 15 000 g for 50 minutes at 4°C. After discarding the supernatant, the pellet was suspended in 250 µL of 2 mM borax buffer, pH 9.3, containing 1% (w/v) BSA and stored at 4°C in the dark.

2.3.2. Preparation of immunochromatographic strips

An immunochromatographic strip is usually composed of a loading area (or sample pad), a detection area and an absorbent pad, the whole being affixed onto a plastic support. The detection area was therefore formed by an antibody-bearing membrane. Migration was supported by two surrounding sample wicking pads made of the same kind of paper than the detection area, free of antibodies and saturated with gelatin (see Figure 1).

2.3.3. Evaluation of the immobilization rate

The test solution was composed of a goat anti-mouse tracer diluted 10 times in the analysis buffer. Papers without antibody

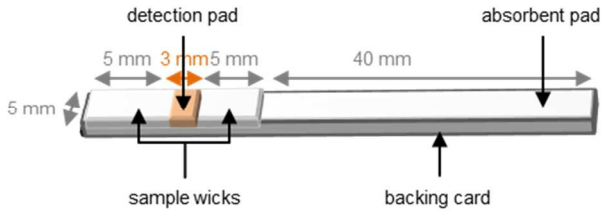

Figure 1: Schematic representation of an immunochromatographic strip.

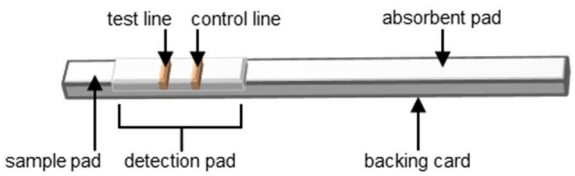

Figure 2: Schematic representation of a "classic" immunochromatographic strip.

in the photoimmobilization solution (ungrafted paper) assessed the unspecific signal due to unspecific adsorption of the tracer onto the detection pad. The immobilization rate of the cellulose papers following the various procedures was measured by the difference between the antibody-grafted paper signal and the ungrafted corresponding one.

2.3.4. Evaluation of the activity rate

Two test solutions were prepared and pre-incubated for 10 minutes. The first one was a solution of OVA and murine anti-OVA mAb tracer (1 µg mL^{-1} and 10-fold dilution, respectively) in the analysis buffer. The second one only contained murine anti-OVA mAb tracer diluted 10 times in the analysis buffer. This immunoassay without antigen (OVA) assessed the unspecific signal due to unspecific adsorption of the tracer onto the antibody–gelatin matrix during immunoassays. The biological activity rate of the grafted antibodies was measured by the difference between the antibody-grafted paper signal in the presence of OVA and the corresponding one in the absence of it.

2.3.5. Determination of the visual detection limit

For this experiment, more "classic" immunochromatographic strips were realized (see Figure 2). These were made of a sample pad, a detection pad and an absorbent pad, all affixed onto the backing card. The detection zone was a paper pad on which anti-mouse antibodies and anti-OVA antibodies (0.5 and 1 mg mL^{-1} in 0.1 M potassium phosphate buffer, pH 7.4, respectively) were automatically dispensed (1 µL cm^{-1}) in two separate lines: control and test line, respectively. This membrane further underwent the photoimmobilization process previously described. It was then fixed to the backing card, along with the absorbent pad above and the sample pad below. These membranes (about 20 cm width) were eventually cut into strips of 5 mm width.

Ten test solutions were prepared and pre-incubated for 15 minutes. The first one only contained murine anti-OVA mAb tracer diluted 10 times in the analysis buffer. This immunoassay without OVA antigen (0 ng mL^{-1}) assessed the unspecific signal due to unspecific adsorption of the tracer onto the antibody-gelatin matrix during immunoassays (negative control). The nine others were solutions of murine anti-OVA mAb tracer (10-time dilution) and OVA (dilution series ranging from 1 ng mL^{-1} to 500 ng mL^{-1}) in the analysis buffer.

The biological activity of the various paper substrates was therefore assessed by the colorimetric difference between the antibody-bearing paper test-line signal in the presence of OVA and the corresponding one without OVA. Since it captured the excess murine anti-OVA tracer antibodies, the control line prevented false negative results. Its coloring guaranteed that the tracer actually passed through the test line, along with the test solution.

The visual detection limit (VDL) was determined through the OVA dilutions series. It was defined as the minimum OVA concentration resulting in a colored signal at the test line significantly more intense than the on the negative control strip.

2.4. Photoimmobilization of probe antibodies

Probe antibodies, or colloidal-gold-labeled antibodies (tracers), were photoimmobilized onto pristine CF1 cellulose paper following the general procedure. CF1 cellulose sheet was impregnated with a goat anti-mouse tracer solution (3-time dilution in the analysis buffer, 20 µL cm^{-2} deposit). Drying step was skipped and this system was then irradiated at 365 nm for 1h20 (about 5 J cm^{-2}). Papers were washed overnight with phosphate buffer containing salts and detergent (0.1M potassium phosphate buffer, pH 7.4, containing 0.5 M NaCl and 0.5% (v/v) Tween 20). Colorimetric measurement using the molecular imager was performed immediately after the paper had been slightly dried over absorbent paper.

3. Results and discussion

3.1. Optimization of immobilization parameters

3.1.1. Photoenergy

Because of the available material (CN-15.LV UV viewing cabinet), various photoenergies could only be obtained by various irradiation times. Therefore a drying phenomenon would add to the irradiation one during long term exposures. In order to get free from that additional factor, a pre-irradiation drying step was applied to all samples.

Anti-OVA antibodies were poured onto CF1 cellulose sheets, and further concentrated by drying the impregnated paper (S). The system was then irradiated (I) at 365 nm for various times, corresponding to different energy levels: 16 min (about 1 J cm^{-2}), 2h40 (about 10 J cm^{-2}) and 21h20 (about 80 J cm^{-2}). Papers were then washed 3 times for 5 minutes with phosphate buffer, saturated and eventually dried. These papers were compared to undried and unirradiated impregnated cellulose (negative control) and to nitrocellulose (positive control) which was assimilated to 100% of antibody immobilization capacity (immobilization rate) and antigen-capture capacity (activity rate). The results corresponding to 2 different immobilizations are presented in Figure 3 and Table 1.

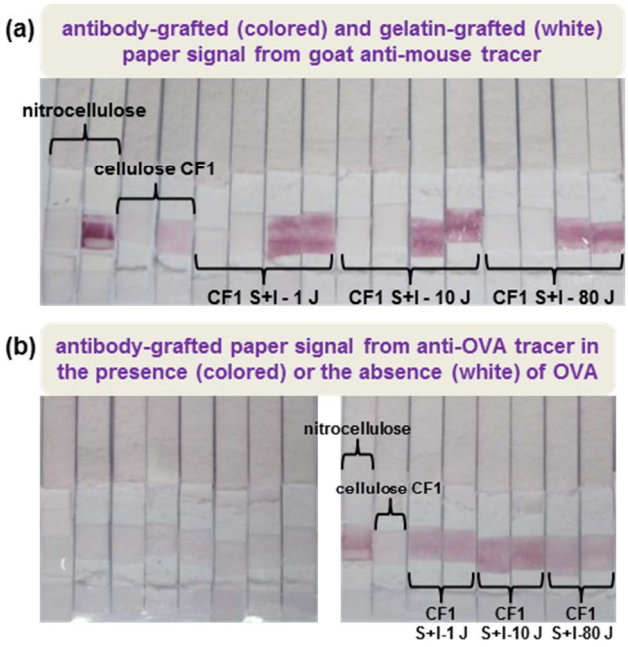

Figure 3: Influence of irradiation energy on antibody immobilization (a) and biological activity (b).
(a) Antibodies immobilized on nitrocellulose or cellulose, after optional drying (S) of the membrane, and irradiation (I) at 1 J cm^{-2}, 10 J cm^{-2} or 80 J cm^{-2}, are revealed by gold-labeled goat anti-mouse tracer antibodies. On ungrafted papers (white/left panel), no signal is detected. On antibody-grafted papers (colored/right panel), performances of nitrocellulose are reached for an irradiation energy of 10 J cm^{-2}. The results corresponding to 2 different immobilizations are shown for each condition.
(b) Antibodies immobilized on nitrocellulose or cellulose, after optional drying (S) of the membrane, and irradiation (I) at 1 J cm^{-2}, 10 J cm^{-2} or 80 J cm^{-2}, are exposed to OVA antigen. The capture of the latter by the immobilized antibodies is highlighted by gold-labeled murine anti-OVA tracer antibodies. In absence of OVA antigen (left panel), no signal is detected. In presence of OVA antigen (right panel), performances of nitrocellulose are reached for an irradiation energy of 10 J cm^{-2}. The results corresponding to 2 different immobilizations are shown for each condition.

Antibodies immobilized onto nitrocellulose or cellulose were revealed by gold-labeled goat anti-mouse tracer antibodies (Figure 3a). On gelatin-grafted papers (white panel), no signal was detected. This absence of unspecific adsorption of tracer molecules proved the gelatin saturation to be effective. On antibody-grafted papers (colored panel), various performances were observed, depending on the photoenergy applied to the system. In the second assay, those immobilized antibodies were exposed to OVA antigen. The capture of the latter by the immobilized antibodies was highlighted by gold-labeled murine anti-OVA tracer antibodies (sandwich immunoassay) (Figure 3b). In absence of OVA antigen (white left panel), no signal is detected. This absence of unspecific adsorption of tracer molecules proved the signal obtained thereafter in presence of OVA to be specific. In presence of OVA antigen (colored right panel), various performances were observed, depending on the photoenergy applied to the system. As can be seen in Table 1, performances of nitrocellulose were reached with an irradiation energy of 10 J cm^{-2}, for both immobilization rate and activity rate.

Table 1: Antibody immobilization and activity rates depending on irradiation energy.

	Specific colorimetric intensity ($\%_{NC}$)	
	Immobilization rate (anti-mouse tracer)	Activity rate (anti-OVA tracer)
Nitrocellulose	100 ± 0.1	100 ± 0.1
Cellulose CF1	29 ± 0.1	31 ± 0.1
CF1 S+I – 1J	85 ± 0.2	69 ± 16
CF1 S+I – 10J	100 ± 3	104 ± 12
CF1 S+I – 80J	76 ± 4	77 ± 9

Antibodies were immobilized on nitrocellulose or cellulose, after optional drying (S) of the membrane, and irradiation (I) at 1 J cm-2, 10 J cm-2 or 80 J cm-2. The results from 2 different immobilizations are presented for each condition.

Table 2: Antibody immobilization and activity rates depending on pre-irradiation drying for short-time irradiation.

	Specific colorimetric intensity ($\%_{NC}$)	
	Immobilization rate (anti-mouse tracer)	Activity rate (anti-OVA tracer)
CF1	25 ± 2	28 ± 7
CF1 I	25 ± 1	8 ± 10
CF1 S+I	68 ± 2	59 ± 6

Antibodies were immobilized onto cellulose, after irradiation (I) or drying and irradiation (S+I), for short irradiation time. The results from 2 different immobilizations are presented for each condition.

Table 3: Antibody immobilization and activity rates depending on pre-irradiation drying for long-time irradiation.

	Specific colorimetric intensity ($\%_{NC}$)	
	Immobilization rate (anti-mouse tracer)	Activity rate (anti-OVA tracer)
CF1	27 ± 6	4 ± 1
CF1 I	88 ± 30	60 ± 6
CF1 S+I	95 ± 3	80 ± 1

Antibodies were immobilized onto cellulose, after irradiation (I) or drying and irradiation (S+I), for long irradiation time. The results from 2 different immobilizations are presented for each condition.

3.1.2. Pre-irradiation drying step

Pre-irradiation drying step was performed in order to concentrate antibodies and therefore bring as many of them as close as possible to cellulose surface. Since the drying phenomenon naturally occurs during long term exposure, the influence of this step was assessed upon both short and long irradiation times.

The CF1 cellulose sheets impregnated with anti-OVA antibodies were either dried (S) or left undried (Ø), irradiated (I) at 365 nm, and then washed with 3 successive 5-minute baths in phosphate buffer. Short irradiation time was 16 min (equivalent to 1 J cm^{-2}), while long irradiation time was 2h40 (equivalent to 10 J cm^{-2}). Resulting immobilization and activity rates were assessed and are shown in Table 2 and Table 3, respectively. According to these graphs, pre-irradiation drying

appears to be required with short irradiation time. Otherwise, antibodies remain in solution, too far away from fibers to be reached by the reactive species and ensure abundant immobilization (see CF1 I samples in Table 2). In addition, its lower performances compared to the negative control (CF1 samples in Table 2) suggest this "long-distance" irradiation of undried substrates to be ineffective. The only immobilization process involved in CF1 I sample would therefore be adsorption, just like in negative control sample. Thus the duration of cellulose exposure to antibody solution is the only real difference between these two samples. As a result, a shorter exposure led to lower performances.

On another hand, pre-irradiation drying seems to be beneficial, although not essential, for long irradiation times (Table 3). As previously noticed, with long irradiation time, drying occurs naturally in the course of irradiation, thereby allowing antibodies to gradually get closer to cellulose surface and to the reactive species.

3.1.3. Post-irradiation washing step

The CF1 cellulose sheets impregnated with anti-OVA antibodies were dried to concentrate the antibodies (S) and then irradiated (I) at 365 nm for 2h40 (about 10 J cm^{-2}). Papers were washed with 3 successive 5-minute baths in either phosphate buffer or phosphate buffer with salts and detergent. The immobilization and activity rates averages with corresponding standard deviations from 3 different experiments are reported in Table 4. Results confirm that extensive washing with a phosphate buffer with salts and detergent allows maintaining on the surface only molecules that are strongly immobilized. Salts allow the electrostatic interactions between biomolecules and surface to be limited, and the detergent reduces or prevents hydrophobic interactions. Salts and detergent thus do contribute to reduce antibody adsorption. The resulting signal therefore appears to be slightly weaker, but results appear to be more reproducible.

3.1.4. Wavelength

The CF1 cellulose sheets impregnated with anti-OVA antibodies were dried to concentrate the antibodies (S) and then either irradiated at 365 nm for 2h40 (I@365), irradiated under visible light for 2h40 (I@visible) or left unirradiated (Ø). Papers were then extensively washed with phosphate buffer containing salts and detergent. The immobilization and activity rates averages with corresponding standard deviations from 3 different experiments are reported in Table 5. As can be seen in this figure, irradiation under visible light provides a slightly less efficient immobilization than irradiation at 365 nm which is more energetic. Visible light could therefore be employed with highly UV-sensitive biomolecules. But for most of antibodies 365-nm irradiation is harmless and would be more efficient.

3.1.5. Optimal procedure

According to previous optimization results, the optimal procedure would be: (i) to impregnate cellulose sheet with an antibody solution; (ii) to concentrate antibodies by drying the impregnated paper at 37°C, in a ventilated oven, for 15 minutes; (iii) to irradiate the system at 365 nm for 2h40 (about 10 J cm^{-2}); and (iv) to intensively wash papers with phosphate buffer containing salts and detergent (0.1M potassium phosphate buffer, pH 7.4, containing 0.5 M NaCl and 0.5% (v/v) Tween 20).

Table 4: Antibody immobilization and activity rates depending on washing solution.

	Specific colorimetric intensity ($\%_{NC}$)	
	Immobilization rate (anti-mouse tracer)	Activity rate (anti-OVA tracer)
CF1 – phosphate buffer	28 ± 2	22 ± 13
CF1 – phosphate buffer with salts & detergent	27 ± 6	4 ± 1
CF1 S+I – phosphate buffer	97 ± 6	106 ± 9
CF1 S+I – phosphate buffer with salts & detergent	95 ± 3	80 ± 1

Antibodies were immobilized onto cellulose, after drying, irradiation (S+I) and washing with phosphate buffer or phosphate buffer with salts and detergent. The results from 3 different immobilizations are presented.

Table 5: Antibody immobilization and activity rates depending on wavelength.

	Specific colorimetric intensity ($\%_{NC}$)	
	Immobilization rate (anti-mouse tracer)	Activity rate (anti-OVA tracer)
CF1	17 ± 5	-2 ± 7
CF1 S+I@365nm	88 ± 5	69 ± 11
CF1 S+I@Visible	69 ± 8	60 ± 0,3

Antibodies were immobilized onto cellulose, after drying (S) and irradiation for 2h40 at either 365 nm (I@365) or under visible light (I@visible). The results from 3 different immobilizations are presented.

Table 6: Antibody immobilization and activity rates depending on paper.

	Specific colorimetric intensity ($\%_{NC}$)	
	Immobilization rate (anti-mouse tracer)	Activity rate (anti-OVA tracer)
CF1	24 ± 10	5 ± 24
CF1 S+I	84 ± 4	76 ± 40
Chr1	21 ± 3	17 ± 12
Chr1 S+I	78 ± 8	103 ± 22
Xerox	15 ± 8	20 ± 5
Xerox S+I	29 ± 5	48 ± 27

Antibodies were immobilized onto various papers according to the optimal procedure. The results from 3 different immobilizations are presented.

3.2. Use of various paper substrates

The versatility of the process was experienced by implementing the optimal procedure to various cellulose paper substrates, namely CF1, Chr1 and Xerox cellulose sheets. CF1 and Chr1 are known as high quality papers, made of quite pure and clean cellulose and commonly used in laboratories (see "Sample Pads for Immunoassays" section [54] and "Cellulose Chromatography Papers" section [55] from Whatman online catalog, respectively).

On another hand, Xerox is a printing paper whose composition is unclear and treatments during papermaking process unknown. The immobilization rate averages with corresponding standard deviations from 3 different experiments are reported in Table 6. Results indicate that the process elaborated in this study allows the observed signal to be increased, with respect to adsorption alone, independently from the nature of the paper. With regard to Xerox paper, the improvement is remarkably low. Xerox paper is most probably treated for being hydrophobic. This would explain why the antibody solution was hindered to penetrate between the fibers, thereby justifying a lower immobilization rate. The process elaborated here was thus proved to allow a larger quantity of functional antibodies to be strongly immobilized on any type of cellulose carrier or derivative.

3.3. Ageing of the membranes

CF1 cellulose sheets were subjected to the optimal procedure and immunochromatographic strips were assembled. A set of strips was immediately tested. Their immobilization and activity rates averages with corresponding standard deviations from 3 different experiments are reported in Table 7 ("fresh" panel). The remaining irradiated cellulose strips, as well as positive control strips, were stored in an oven for 7 days at 40°C in order to assess the ageing effects on the prepared membranes. Their immobilization and activity rates averages with corresponding standard deviations from 3 different experiments are reported in Table 7 ("1-week old" panel). According to these results, ageing of nitrocellulose-based membranes results in a decreased recognition of the grafted antibodies by the goat anti-mouse tracer, as well as in a reduced biological activity. This phenomenon may be explained by the denaturation of the immobilized antibodies. With regard to cellulose-based membranes, signal variability increases with ageing while recognition by goat anti-mouse tracer decreases and may also result from the denaturation of immobilized antibodies. Nevertheless, the observed decrease is less important with cellulose than with nitrocellulose: $\delta(\text{immobilization})_{\text{nitrocellulose}}$ = -20% *vs* $\delta(\text{immobilization})_{\text{cellulose}}$ = -11%. Moreover, the activity rate of cellulose-based membranes remains constant after accelerated ageing, when standard deviations are considered. This may suggest that the binding sites of the antibodies photoimmobilized onto cellulose are not damaged. Another hypothesis would be that the active antibodies are protected from damage because they are "buried" and hidden in the paper substrate whereas they are displayed and vulnerable on the nitrocellulose surface. Cellulose immunoassay membranes prepared according to the process presented here thus appear to be more ageing resistant than nitrocellulose ones, and are therefore more suitable for use after long storage.

3.4. Membranes performances

Membranes performance was evaluated in terms of visual detection limit (VDL). To this end, more "classic" immunochromatographic strips were realized (see section 2.3.5). After antibody solutions had been dispensed onto the substrates, the antibodies were either adsorbed onto nitrocellulose or photoimmobilized onto cellulose. First, their immobilization was confirmed by revelation with gold-labeled goat anti-mouse tracer (see control strips in Figure 4). Then, their biological activity was put to the test by exposition to OVA antigen and simultaneously revealed by gold-labeled murine anti-OVA tracer (sandwich immunoassay) (see OVA strips in Figure 4). They were tested through an OVA dilution series ranging from 0 ng mL^{-1} (negative control) to 500 ng mL^{-1} (positive control). Each test was performed in triplicate.

Photoimmobilization onto cellulose led to VDL results in the same order of magnitude as the values obtained with adsorption onto nitrocellulose which is the reference process. However, cellulose performances appeared slightly lower than nitrocellulose's ($VDL_{\text{cellulose}}$=5 $VDL_{\text{nitrocellulose}}$). Beyond procedure, this phenomenon might stem from the many differences both chemical and physical between the two substrates. Indeed, in addition to the obvious chemical difference in molecular structure, the main physical difference between nitrocellulose and cellulose substrates lies in their porosity (about 5 µm and 11 µm surface pore size, respectively)

Table 7: Antibody immobilization and activity rates depending on ageing.

	Specific colorimetric intensity ($\%_{NC}$)	
	Immobilization rate (anti-mouse tracer)	Activity rate (anti-OVA tracer)
CF1 – fresh	17 ± 5	-2 ± 7
Nitrocellulose – fresh	100 ± 0,1	100 ± 0,1
CF1 S+I – fresh	88 ± 5	69 ± 11
Nitrocellulose – 1-week old	80 ± 0,1	61 ± 0,1
CF1 S+I – 1-week old	78 ± 8	72 ± 15

Antibodies were immobilized onto cellulose according to the optimal procedure. Fresh and aged strips were compared. The results from 3 different samples are presented.

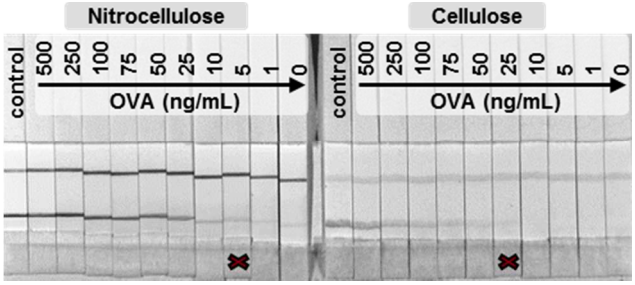

Figure 4: Photographs showing the influence of the immobilization process and the membrane material on biological activity and VDL. Antibodies were adsorbed onto nitrocellulose and photoimmobilized onto cellulose. Their actual immobilization was confirmed thanks to gold-labeled goat anti-mouse tracer (control strips). The capture of OVA antigen by the immobilized antibodies was highlighted by gold-labeled murine anti-OVA tracer (OVA strips). The strips corresponding to the membranes' VDL are labeled with a cross. Photographs were taken with the Molecular Imager. All experiments were reproduced 3 times but only one is shown here.

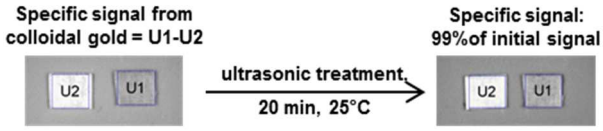

Figure 5: Photoimmobilization of gold-labeled goat anti-mouse tracer antibodies. Photograph was taken with VersaDoc™ Molecular Imager.

and sheet thickness (20 µm and 176 µm thick, respectively). Unfortunately, cellulose sheets with same porosity and thickness than nitrocellulose were not commercially available. Therefore we are not able to prove yet that the physical difference might be mainly responsible for the signal variation.

3.5. Strength of the immobilization

In order to assess the strength of the photoimmobilization, probe antibodies were immobilized according to the procedure described in section 2.4. After a first colorimetric measurement, the probe-antibody-bearing paper was then immersed in phosphate buffer containing salts and detergent (0.1M potassium phosphate buffer, pH 7.4, containing 0.5 M NaCl and 0.5% (v/v) Tween 20) and subjected to ultrasonic treatment for 20 minutes. Colorimetric intensity was measured again. The colorimetric intensity measured after the ultrasonic treatment amounts to about 99% of the first intensity measured (Figure 5). Considering that the observed signal decrease is comprised within the measuring error deviation, this decrease can therefore be considered as non-significant. In conclusion, the immobilization resulting from the process developed in this study is thus very strong, or even covalent.

3.6. Proposed mechanism

Several studies may raise suggestions about the possible mechanism. Particularly, accelerated photo-ageing experiments demonstrated that cellulose exposure to long-scale UV and visible light ($\lambda \geq 340$ nm) induced extensive oxidative degradation of cellulose, along with formation of hydroxyl radicals and carbonyl groups. Photooxidative reactions resulted in an increase of carbonyl, carboxyl and hydroperoxide content. The species described in that study are depicted in Supplementary Information (SI-Figure 8) [56]. Furthermore, another study showed that carbonyl groups resulting from cellulose exposure to 254-nm UV light condensed with primary amino groups from species previously poured onto cellulose to form imines (see SI-Figure 9 in Supplementary Information). This phenomenon would be responsible for the yellowing of cellulose papers treated with amino compounds [57], which yellowing also occurs under natural light exposure ($\lambda \geq 280$ nm). To the best of our knowledge, no study has proved this imine formation under 365-nm UV light thus far. However, this is well conceivable given that carbonyl groups are produced during accelerated photo-ageing of cellulose at this same wavelength [56]. In addition these carbonyl groups are easily condensed with primary amines from biomolecules under mild conditions. This is actually a broadly used method for chemically immobilize biomolecules onto cellulose [58].

In light of those readings, two mechanisms could be proposed for the photolinker-free photoimmobilization process presented herein: an oxidative mechanism involving carbonyl moieties (Figure 6a) and a radical mechanism (Figure 6b). If the carbonyl mechanism (Figure 6a) actually occurred, nearly no difference should be observed by irradiating the substrate prior to antibody deposit. This verification experiment had been conducted (results not shown) and led to both immobilization rate and activity rate similar to the negative control (pristine unirradiated cellulose paper) values. The carbonyl mechanism was therefore excluded and the radical mechanism (Figure 6b) seemed to be the most likely. Besides, the latter would be consistent with both the need for antibody concentration observed during optimization experiments and the results observed with cellulose pre-irradiation aforementioned. Indeed, radicals have a short lifetime related to a high reactivity and therefore react in short range. Hence, the radicals created by pre-irradiation would have been degraded before the antibody deposit and would lead to results similar to unirradiated papers (above result). In addition, radicals would only react with the

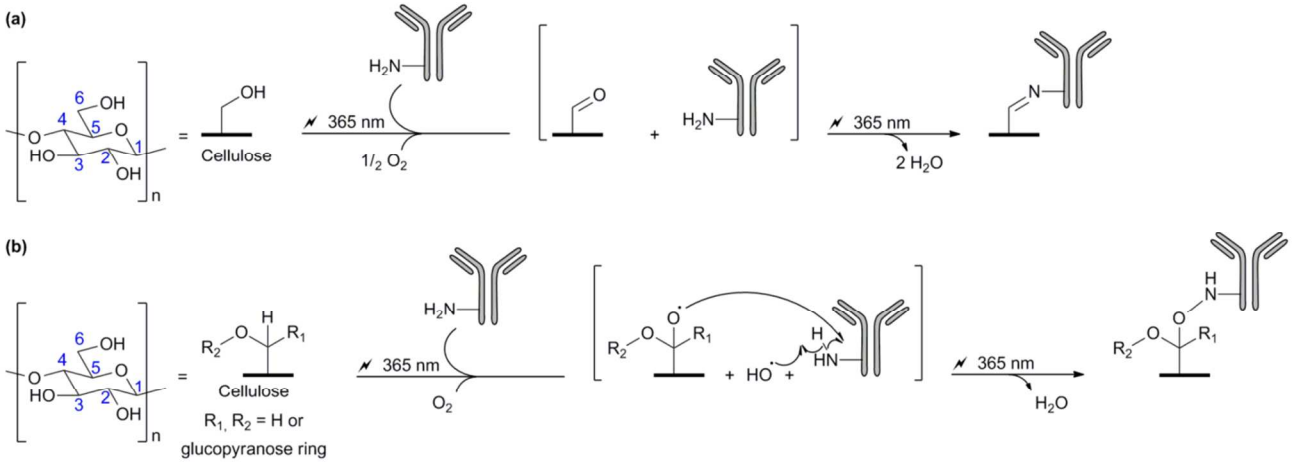

Figure 6: Proposed mechanisms for photoimmobilization of antibodies onto cellulose. The oxidative mechanism (a) is based on references [57,56,58], while the radical mechanism (b) is only based on reference [56].

closest antibodies which are many more after a concentration step (optimization result). More experiments such as ESR are in progress in order to confirm this hypothesis.

4. Conclusion

A photolinker-free photografting procedure for antibody immobilization onto cellulose has been described. This whole new method allows biomolecules to be immobilized onto cellulose without any photocoupling intermediate nor any biomolecule or substrate pretreatment. This process is therefore fast, simple, cost-saving and environmentally-friendly. Various parameters of the photoimmobilization process have been optimized, therefore resulting in an optimal procedure which produces membranes challenging nitrocellulose performances. This research aimed at fulfilling the need for cost-saving and rapid methods allowing robust, abundant and sustainable binding of biomolecules onto cellulose sheets. In addition to the obvious advantages of a photolinker-free process, cellulose is an almost inexhaustible raw material with large bioavailability and good biodegradability. More generally, the expounded process provides a powerful tool for immobilizing chemical-sensitive biomolecules onto cellulose sheets.

Acknowledgements

This work was financially supported by the Commissariat à l'Energie Atomique et aux Energies Alternatives (France).

Notes and references

[a] CEA Saclay, IRAMIS, NIMBE, LICSEN (Laboratory of Innovation in Surface Chemistry and Nanosciences), F-91191 Gif sur Yvette, France; E-mails: julie.credou@cea.fr; thomas.berthelot@cea.fr.
[b] CEA Saclay, iBiTec-S, SPI, LERI (Laboratory of Study and Research in Immunoanalysis), F-91191 Gif sur Yvette, France; E-mail: herve.volland@cea.fr.
* Author to whom correspondence should be addressed; E-mail: thomas.berthelot@cea.fr; Tel.: +33 169086588; Fax: +33 169084044.

1. A. W. Martinez, S. T. Phillips, G. M. Whitesides, and E. Carrilho, *Anal. Chem.*, 2010, **82**, 3–10.
2. L. Ge, J. Yan, X. Song, M. Yan, S. Ge, and J. Yu, *Biomaterials*, 2012, **33**, 1024–1031.
3. C.-M. Cheng, A. W. Martinez, J. Gong, C. R. Mace, S. T. Phillips, E. Carrilho, K. A. Mirica, and G. M. Whitesides, *Angew. Chem. Int. Ed. Engl.*, 2010, **49**, 4771–4774.
4. J. Hu, S. Wang, L. Wang, F. Li, T. J. Lu, and F. Xu, *Biosens. Bioelectron.*, 2014, **54**, 585–597.
5. S. Wiriyachaiporn, P. H. Howarth, K. D. Bruce, and L. A. Dailey, *Diagn. Microbiol. Infect. Dis.*, 2013, **75**, 28–36.
6. J. M. Gonzalez, M. W. Foley, N. M. Bieber, P. A. Bourdelle, and R. S. Niedbala, *Anal. Bioanal. Chem.*, 2011, **400**, 3655–3664.
7. D. D. Liana, B. Raguse, J. J. Gooding, and E. Chow, *Sensors*, 2012, **12**, 11505–11526.
8. A. K. Yetisen, M. S. Akram, and C. R. Lowe, *Lab Chip*, 2013, **13**, 2210–2251.
9. G. Zhou, X. Mao, and D. Juncker, *Anal. Chem.*, 2012, **84**, 7736–7743.
10. H. Anany, W. Chen, R. Pelton, and M. W. Griffiths, *Appl. Environ. Microbiol.*, 2011, **77**, 6379–6387.
11. S. M. Zakir Hossain, R. E. Luckham, M. J. McFadden, and J. D. Brennan, *Anal. Chem.*, 2009, **81**, 9055–9064.
12. M. Vaher and M. Kaljurand, *Anal. Bioanal. Chem.*, 2012, **404**, 627–633.
13. R. S. J. Alkasir, M. Ornatska, and S. Andreescu, *Anal. Chem.*, 2012, **84**, 9729–9737.
14. S. M. Zakir Hossain, C. Ozimok, C. Sicard, S. D. Aguirre, M. M. Ali, Y. Li, and J. D. Brennan, *Anal. Bioanal. Chem.*, 2012, **403**, 1567–1576.
15. M. Zhang, L. Ge, S. Ge, M. Yan, J. Yu, J. Huang, and S. Liu, *Biosens. Bioelectron.*, 2013, **41**, 544–550.
16. C. Sicard and J. D. Brennan, *MRS Bull.*, 2013, **38**, 331–334.
17. J. Kirsch, C. Siltanen, Q. Zhou, A. Revzin, and A. Simonian, *Chem. Soc. Rev.*, 2013, **42**, 8733–8768.
18. S. B. Murugaiyan, R. Ramasamy, N. Gopal, and V. Kuzhandaivelu, *Adv. Biomed. Res.*, 2014, **3**, 67.
19. L. Berrade, A. E. Garcia, and J. a Camarero, *Pharm. Res.*, 2011, **28**, 1480–1499.
20. A. Foudeh, T. Fatanat-Didar, T. Veres, and M. Tabrizian, *Lab Chip*, 2012, **12**, 3249–3266.
21. X. Li, D. R. Ballerini, and W. Shen, *Biomicrofluidics*, 2012, **6**, 011301.
22. P. Jonkheijm, D. Weinrich, H. Schröder, C. M. Niemeyer, and H. Waldmann, *Angew. Chem. Int. Ed. Engl.*, 2008, **47**, 9618–9647.
23. T. R. J. Holford, F. Davis, and S. P. J. Higson, *Biosens. Bioelectron.*, 2011, **34**, 12–24.
24. A. H. Peruski and L. F. Peruski, *Clin. Vaccine Immunol.*, 2003, **10**, 506–513.
25. G. A. Posthuma-Trumpie, J. Korf, and A. van Amerongen, *Anal. Bioanal. Chem.*, 2009, **393**, 569–582.
26. R. Hawkes, E. Niday, and J. Gordon, *Anal. Biochem.*, 1982, **119**, 142–147.
27. B. Ngom, Y. Guo, X. Wang, and D. Bi, *Anal. Bioanal. Chem.*, 2010, **397**, 1113–1135.
28. R. C. Wong and H. Y. Tse, *Lateral Flow Immunoassay*, Humana Press, New York, NY, 2009.
29. R. W. Peeling and D. Mabey, *Clin. Microbiol. Infect.*, 2010, **16**, 1062–1069.
30. P. von Lode, *Clin. Biochem.*, 2005, **38**, 591–606.
31. J. Burstein and G. D. Braunstein, *Early Pregnancy*, 1995, **1**, 288–296.
32. T. Chard, *Hum. Reprod.*, 1992, **7**, 701–710.
33. F. Kong and Y. F. Hu, *Anal. Bioanal. Chem.*, 2012, **403**, 7–13.
34. G. E. Fridley, C. A. Holstein, S. B. Oza, and P. Yager, *MRS Bull.*, 2013, **38**, 326–330.
35. Millipore Corporation, *Millistak+ HC Filter Devices (with RW01); MSDS No. M114480*, Millipore Corporation, Billerica, MA, USA, 2008.
36. Millipore Corporation, *Nitrocellulose Membrane Filters; MSDS No. 00000100SDS*, Millipore Corporation, Billerica, MA, USA, 2011.
37. J. Credou, H. Volland, J. Dano, and T. Berthelot, *J. Mater. Chem. B*, 2013, **1**, 3277–3286.
38. J. Credou and T. Berthelot, *J. Mater. Chem. B*, 2014. DOI: 10.1039/C4TB00431K.

39. J. S. Han and J. S. Rowell, in *Paper and composites from agro-based resources*, eds. R. M. Rowell, R. A. Young, and J. K. Rowell, CRC Press, 1996, pp. 83–134.
40. D. Klemm, B. Heublein, H.-P. Fink, and A. Bohn, *Angew. Chem. Int. Ed. Engl.*, 2005, **44**, 3358–3393.
41. S. Kalia, B. S. Kaith, and I. Kaur, *Cellulose Fibers: Bio- and Nano-Polymer Composites*, Springer Berlin Heidelberg, Berlin, Heidelberg, 2011.
42. D. Klemm, F. Kramer, S. Moritz, T. Lindström, M. Ankerfors, D. Gray, and A. Dorris, *Angew. Chem. Int. Ed. Engl.*, 2011, **50**, 5438–5466.
43. B. A. Kerwin and R. L. Remmele, *J. Pharm. Sci.*, 2007, **96**, 1468–1479.
44. P. Viel, J. Walter, S. Bellon, and T. Berthelot, *Langmuir*, 2013, **29**, 2075–2082.
45. H. Volland, P. Pradelles, F. Taran, L. Buscarlet, and C. Creminon, *J. Pharm. Biomed. Anal.*, 2004, **34**, 737–752.
46. G. T. Hermanson, *Bioconjugate techniques*, Academic Press, London, 2008.
47. P. Tingaut, R. Hauert, and T. Zimmermann, *J. Mater. Chem.*, 2011, **21**, 16066–16076.
48. S. Kumar and P. Nahar, *Talanta*, 2007, **71**, 1438–1440.
49. U. Bora, P. Sharma, K. Kannan, and P. Nahar, *J. Biotechnol.*, 2006, **126**, 220–229.
50. U. Bora, K. Kannan, and P. Nahar, *J. Memb. Sci.*, 2005, **250**, 215–222.
51. J. Credou and T. Berthelot, 2014. EP14157944.
52. N. Khreich, P. Lamourette, P.-Y. Renard, G. Clavé, F. Fenaille, C. Créminon, and H. Volland, *Toxicon*, 2009, **53**, 551–559.
53. N. Khreich, P. Lamourette, H. Boutal, K. Devilliers, C. Créminon, and H. Volland, *Anal. Biochem.*, 2008, **377**, 182–188.
54. Whatman GE Healthcare, *Sample Pads for Immunoassays*. http://www.gelifesciences.com/webapp/wcs/stores/servlet/catalog/fr/GELifeSciences-fr/products/AlternativeProductStructure_23129/ (accessed May 27, 2014).
55. Whatman GE Healthcare, *Cellulose Chromatography Papers*. http://www.gelifesciences.com/webapp/wcs/stores/servlet/catalog/fr/GELifeSciences-fr/products/AlternativeProductStructure_21507/ (accessed May 27, 2014).
56. J. Malešič, J. Kolar, M. Strlič, D. Kočar, D. Fromageot, J. Lemaire, and O. Haillant, *Polym. Degrad. Stab.*, 2005, **89**, 64–69.
57. M. U. de la Orden and J. Martínez Urreaga, *Polym. Degrad. Stab.*, 2006, **91**, 2053–2060.
58. S. Wang, L. Ge, X. Song, M. Yan, S. Ge, J. Yu, and F. Zeng, *Analyst*, 2012, **137**, 3821–3827.

Table of contents entry

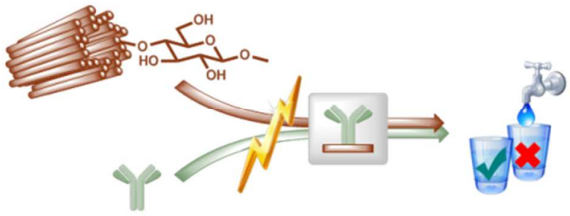

Immunoassay membranes were produced by photoimmobilization of antibodies onto cellulose without any photocoupling intermediate nor any biomolecule or substrate pretreatment.